# Quantum-phase dynamics of molecular systems interacting with a two-mode squeezed vacuum field: Detuning effects

**ARTICLE** *in* INTERNATIONAL JOURNAL OF QUANTUM CHEMISTRY · SEPTEMBER 2004

Impact Factor: 1.43 · DOI: 10.1002/qua.10865



**2 AUTHORS**, INCLUDING:

Masayoshi Nakano
Osaka University
**337** PUBLICATIONS **4,781** CITATIONS

SEE PROFILE

# Quantum-Phase Dynamics of Molecular Systems Interacting with a Two-Mode Squeezed Vacuum Field: Detuning Effects

**M. NAKANO, K. YAMAGUCHI**

*Department of Chemistry, Graduate School of Science, Osaka University, Toyonaka, Osaka 560-0043, Japan*

*Received 11 December 2002; accepted 10 October 2003*
*Published online 18 February 2004 in Wiley InterScience (www.interscience.wiley.com).*
*DOI 10.1002/qua.10865*

**ABSTRACT:** We investigated several three-state molecular models interacting with an on/off-resonant two-mode squeezed vacuum field (TSV) to clarify the detuning effects on the dynamic behaviors of on/off-diagonal molecular density matrices. For comparison, we perform a parallel study in which the initial field is an on/off-resonant two-mode coherent field. In the case of satisfying both a large one-photon detuning and a two-photon resonance conditions, the magnitude of off-diagonal density matrix ($|\rho_{13}|$) between the second excited and the ground states for (TSV) exhibits distinct increase and decrease behaviors similar to the case of a two-mode coherent field in contrast to the case of one- and two-photon resonances, in which a random oscillation of $|\rho_{13}|$ with a relatively high averaged value is observed. The change in the contribution of one- and two-photon processes due to the detuning of external fields and the differences in the quantum statistics of the initial quantum fields are found to cause such attractive variations in dynamics of the coherency between molecular electronic states as well as their populations.  Int J Quantum Chem 99: 421–430, 2004

**Key words:** squeezed field; Pegg–Barnett phase; detuning effect; quantum dynamics

*Correspondence to:* M. Nakano; e-mail: mnaka@cheng.es.osaka-u.ac.jp

M. Nakano's present address is Division of Chemical Engineering, Department of Materials Engineering, Graduate School of Engineering Science, Osaka University, Toyonaka, Osaka 560-8531, Japan.

## Introduction

The dynamics of atoms/molecules interacting with quantized photon fields is known to provide various attractive phenomena in which pure quantum features play an important role [1–22]. Previously [23–29], we studied the coherency dynamics of molecular electronic states coupled with a squeezed field [26, 27], which exhibits remarkable nonclassic features [30] and is applicable in quantum computer and quantum nondemolition detection. Recently, much attention has been directed to the consideration of the interaction between atoms/molecules and two-mode squeezed photon fields although these experimental realizations have not yet been achieved. Several interesting features have been elucidated in the effect of initial intermode field correlations, the degree of which is measured by the information entropy [31], for example, of two-mode squeezed vacuum (TSV) field [32] on the system dynamics [33, 34]. The TSV field is known to be a highly nonclassic state of the photon field, in which the individual modes display random thermal fluctuations although a superposition of the modes exhibits a reduction in noise below the quantum limit [35]. This feature is also utilized in thermofield dynamics [36, 37]. We investigated the relations between molecular population dynamics and photon-phase dynamics in the systems composed of three-state molecular models and several kinds of dynamic features of such model systems remarkably depend on the initial photon-number and -phase distributions of two-mode fields. Our previous study on a three-sate molecular system interacting with a resonant TSV has also clarified that the off-diagonal density matrix between the ground and second excited states preserves large values similarly to the case of a two-mode coherent field although other density matrices vanish like a thermal field. In general, the detuning of external quantized fields is known to remarkably affect the dynamics of atomic populations [33]. In this study, therefore, we investigated the effects of detuning on the dynamics of photon-phase distributions [calculated by the Pegg–Barnett (PB) phase operator] and the coherency between molecular states (described by the off-diagonal molecular density matrices) using a three-state molecular system interacting with an on/off-resonant TSV field. For comparison, the dynamics of the molecular systems interacting with an on/off-resonant two-mode coherent field is also investigated.

## Methodology

### MODEL HAMILTONIAN AND A PROCEDURE OF DYNAMICS

The Hamiltonian for a molecular model with $M$ states ($M \geq 2$: integer) interacting with a two-mode photon field under the dipole approximation is represented by

$$\begin{aligned} H &= H_{\mathrm{mol}} + H_{\mathrm{field}} + H_{\mathrm{int}} \\ &= \sum_{i}^{M} E_i a_i^+ a_i + \sum_{\lambda}^{2} \left( b_\lambda^+ b_\lambda + \frac{1}{2} \right) \hbar\omega_\lambda \\ &\quad + \sum_{i,j}^{M} \sum_{\lambda}^{2} \left( \frac{\hbar\omega_\lambda}{2\varepsilon_0 V} \right)^{1/2} d_{ij} a_i^+ a_j (b_\lambda^+ + b_\lambda), \quad (1) \end{aligned}$$

where $H_{\mathrm{mol}}$ is the Hamiltonian of the nonperturbed molecular system, $H_{\mathrm{field}}$ is the Hamiltonian of the two-mode photon field, and $H_{\mathrm{int}}$ is the interaction Hamiltonian. $E_i$ represents the energy of the molecular electronic state $i$, and $a_i^+$ and $a_i$ are, respectively, the creation and annihilation operators for the quantized electron field in the $i$th energy state. $\omega_\lambda$ indicates the frequency of photon mode $\lambda$ and $b_\lambda^+$ and $b_\lambda$ are the creation and annihilation operators, respectively, for photon mode $\lambda$. The $d_{ij}$ is the matrix element of the molecular dipole moment operator in the direction of the polarization of photon field. It is assumed that the polarization vector of each mode coincides with each other. $V$ is the volume of the cavity containing the photon field, and it is fixed to $10^7$ Å$^3$ in this study. Note that the quantities $E_{ij}$ and $d_{ij}$ concerning electronic states of a molecule are calculated in advance using appropriate quantum chemical methods. The matrix elements of the above Hamiltonian using a triple Hilbert space basis, $|j; n_1, n_2\rangle$ ($\equiv |j\rangle \otimes |n_1\rangle \otimes |n_2\rangle$) (molecular states $\{|j\rangle\}$ ($j = 1, 2, \ldots, M$) and the photon-number states of modes 1 and 2, i.e., $\{|n_1\rangle\}$ and $\{|n_2\rangle\}$ ($n_1, n_2 = 0, 1, 2, \ldots, \infty$)), are presented in our previous article [38].

Using the matrix elements of time-evolution operator $U(t, t_0)$ [23–29] represented by eigenvalues $\{W(m)\}$ and eigenvectors $\{\chi(m)\}$ ($m = 0, 1, 2, \ldots$) of the Hamiltonian [Eq. (1)], the elements of density matrix are represented by

$$\langle j;\, n_1,\, n_2|\rho(t)|j';\, n_1',\, n_n'\rangle \equiv \rho_{j,n_1,n_2;\,j',n_1',n_2'}(t)$$

$$= \sum_{f,g}^{M} \sum_{\substack{m_1,m_2,\\ m_1',m_2'}} U_{j,n_1,n_2;f,m_1,m_2}(t,\, t_0)\rho_{f,m_1,m_2;g,m_1',m_2'}(t_0)$$

$$U^{+}_{g,m_1',m_2';\,j',n_1',n_2'}(t,t_2). \quad (2)$$

The molecule is assumed to be in the ground state at the initial time. As the initial photon field, two types of two-mode photon fields, i.e., a two-mode coherent field (TC) and a TSV field, are considered. The explicit form of density matrix elements of TC are given in our previous articles [23–29]. In contrast to TC, TSV is a correlated two-mode field so it cannot be represented by the direct product of each one-mode density matrix. For two modes 1 and 2 with annihilation operators $b_1$ and $b_2$, the state of (TSV), $|\zeta\rangle$, is given by [39]

$$|\zeta\rangle = \hat{S}_{12}(\zeta)|0;\, 0\rangle$$

$$= \text{sech } r \sum_n [-\exp(i\varphi)\tanh r]^n |n_1;\, n_2\rangle, \quad (3)$$

where

$$\hat{S}_{12}(\zeta) = \exp(\zeta^* b_1 b_2 - \zeta b_1^+ b_2^+). \quad (4)$$

Here, $\zeta = re^{i\varphi}$ is any complex number with modulus $r$ and argument $\varphi$, which determine the squeezing intensity and the direction of squeezing, respectively. The field $|\zeta\rangle$ is an entangled state between modes 1 and 2, and is not the product of a state for mode 1 and one for mode 2. It is noted that the one-mode properties of each of TSV, $|\zeta\rangle$, are precisely those of a one-mode thermal field [39]. The density matrix elements of TSV are obtained by $\rho^{\text{2photo}}_{m_1,m_2;m_1';m_2'} = \langle m_1,\, m_2|\zeta\rangle\langle\zeta|m_1',\, m_2'\rangle)$ using Eq. (3). The density matrix elements $[\rho_{j,n_1,n_2;j',n_1',n_2'}(t)]$ at time $t$ are obtained using Eq. (2) and then several reduced density matrix elements are calculated by

$$\rho^{\text{mol}}_{f,g}(t) = \sum_{m_1,m_2} \rho_{f,m_1,m_2;g,m_1,m_2}(t)$$

(molecular density), (5)

$$\rho^{\text{2phot}}_{m_1,m_2;m_1',m_2'}(t) = \sum_f \rho_{f,m_1,m_2;f,m_1',m_2'}(t)$$

(two-mode photon-field density), (6)

$$\rho^{\text{1phot}}_{m_1,m_1'}(t) = \sum_{m_2} \rho^{\text{2phot}}_{m_1,m_2;m_1',m_2}(t)$$

(one-mode photon-field density for mode 1), (7)

and

$$\rho^{\text{1phot}}_{m_2,m_2'}(t) = \sum_{m_1} \rho^{\text{2phot}}_{m_1,m_2;m_1,m_2'}(t)$$

(one-mode photon-field density for mode 2). (8)

Various properties concerning the molecule and photons are calculated using these reduced density matrices.

## TWO-MODE PB PHASE OPERATOR

Because the definition and detailed explanations of two-mode PB phase operator [40–42] have been given in previous articles [23–29, 43], we just provide the results of the two-mode photon-phase distribution functions:

$$P(\phi^1_{m_1},\, \phi^2_{m_2}) = \frac{1}{(s+1)^2} \sum_{\substack{n_1,n_2,\\ n_1',n_2'}} \rho^{\text{2phot}}_{n_1,n_2;n_1',n_2'} e^{i(n_1'-n_1)\phi^1_{m_1}} e^{i(n_2'-n_2)\phi^2_{m_2}}. \quad (9)$$

Here, $\phi^i_m = \phi^i_0 + 2\pi m/(s+1)$ $(m = 0, 1, \ldots, s)$ and $\phi^i_0 = -s\pi/(s+1)$, where $s$ is taken to be 100 in this study. The phase-sum $P(\phi^+_m)(\equiv P(\phi^1_{m_1} + \phi^2_{m_2}))$ and phase-difference $P(\phi^-_m)(\equiv P(\phi^2_{m_2} - \phi^1_{m_1}))$ distributions are, respectively, represented by

$$P(\phi^+_m) = \frac{1}{(s+1)} \sum_{n_1,n_2} \sum_{n_1'} \rho^{\text{2phot}}_{n_1',(n_1'-n_1+n_2);n_1,n_2} e^{i(n_1-n_1')\phi^+_m} \quad (10)$$

and

$$P(\phi^-_m) = \frac{1}{(s+1)} \sum_{n_1,n_2} \sum_{n_1'} \rho^{\text{2phot}}_{n_1',(n_1-n_1'+n_2);n_1,n_2} e^{i(n_1'-n_1)\phi^-_m}. \quad (11)$$

We can also derive the one-mode photon-phase distribution $P(\phi^\lambda_{m_\lambda})$ $(\lambda = 1, 2)$ using Eqs. (10) and (11) as follows:

$$P(\phi^\lambda_{m_\lambda}) = \frac{1}{s+1} \sum_{n_\lambda,n_\lambda'} \rho^{\text{1phot}}_{n_\lambda,n_\lambda} e^{i(n_\lambda-n_\lambda')\phi_m} \quad (\lambda = 1, 2). \quad (12)$$

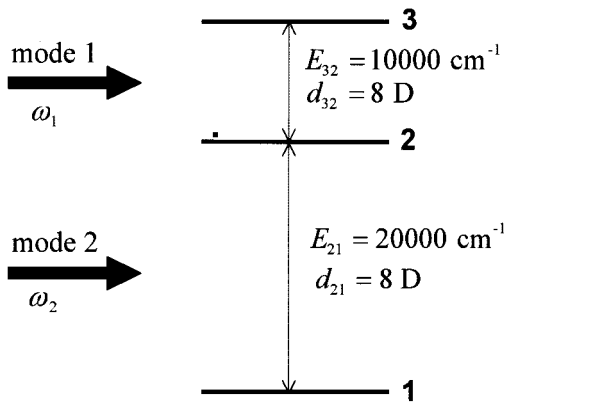


(TC) Two-mode coherent field
(TC-a) $\omega_1 = 10000$ cm$^{-1}$, $\omega_2 = 20000$ cm$^{-1}$
(TC-b) $\omega_1 = 10200$ cm$^{-1}$, $\omega_2 = 19800$ cm$^{-1}$
(TC-c) $\omega_1 = 10300$ cm$^{-1}$, $\omega_2 = 19700$ cm$^{-1}$
(TC-d) $\omega_1 = 10400$ cm$^{-1}$, $\omega_2 = 19600$ cm$^{-1}$

(TSV) Two-mode squeezed vacuum field
(TSV-a) $\omega_1 = 10000$ cm$^{-1}$, $\omega_2 = 20000$ cm$^{-1}$
(TSV-b) $\omega_1 = 10200$ cm$^{-1}$, $\omega_2 = 19800$ cm$^{-1}$
(TSV-c) $\omega_1 = 10300$ cm$^{-1}$, $\omega_2 = 19700$ cm$^{-1}$
(TSV-d) $\omega_1 = 10400$ cm$^{-1}$, $\omega_2 = 19600$ cm$^{-1}$

**FIGURE 1.** Three-state molecular model interacting with a two-mode photon field. The transition moments are $d_{21} = 8.0$ D and $d_{32} = 8.0$ D. $\omega_1$ and $\omega_2$ are the frequencies of two-mode fields, the sum of which is resonant with the energy interval $E_{31} = 30{,}000$ cm$^{-1}$. The four types of ($\omega_1$, $\omega_2$)—(a) (10,000 cm$^{-1}$, 20,000 cm$^{-1}$), (b) (10,200 cm$^{-1}$, 19,800 cm$^{-1}$), (c) (10,300 cm$^{-1}$, 19,700 cm$^{-1}$), and (d) (10,400 cm$^{-1}$, 19,600 cm$^{-1}$)—are considered. We consider two types of photon fields, i.e., TC and TSV. The considered models are represented by the external field and frequencies, e.g., TC-a. The initial average photon number of each mode is 4.

## Results and Discussion

### PHOTON-NUMBER AND -PHASE DISTRIBUTIONS OF INITIAL TWO-MODE FIELDS

Figure 1 shows the three-state model considered in this study. The energy intervals are assumed to be $E_{21}(\equiv E_2 - E_1) = 20{,}000$ cm$^{-1}$ and $E_{32}(\equiv E_3 - E_2) = 10{,}000$ cm$^{-1}$, and the transition moments along the polarization of external fields are $d_{21} = 8$ D and $d_{32} = 8$ D. The two types of two-mode fields, i.e., TC and TSV, have several kinds of frequencies: (a) $\omega_1 = 10{,}000$ cm$^{-1}$ and $\omega_2 = 20{,}000$ cm$^{-1}$, (b) $\omega_1 = 10{,}200$ cm$^{-1}$ and $\omega_2 = 19{,}800$ cm$^{-1}$, (c) $\omega_1 = 10{,}300$ cm$^{-1}$ and $\omega_2 = 19{,}700$ cm$^{-1}$, and (d) $\omega_1 = 10{,}400$ cm$^{-1}$ and $\omega_2 = 196{,}000$ cm$^{-1}$. The considered model is represented by the applied field and its frequency, e.g., TC-a. All these fields are two-photon ($\omega_1 + \omega_2$) resonant with $E_{31}$ of the three-state model (see Fig. 1), while the detuning (off-resonancy) of one-photon process with respect to the intermediate state **2** increases from (2) to (4), namely, we can obtain the one-photon detuning effects on the dynamics from these results.

The average photon number of each mode is fixed to $\langle \hat{n}_1 \rangle = \langle \hat{n}_2 \rangle = 4$ at the initial time. The squeezing parameters of TSV are $r = \sinh^{-1} \sqrt{\langle \hat{n}_1 \rangle} \approx 1.443635475$ [43] and $\varphi = 0$. Note that the one-mode photon-phase and one-mode photon-number distributions for the two modes of these fields are identical with each other at the initial time, respectively: $P(n_1) = P(n_2)(\equiv P(n))$ and $P(\phi^1_{m_1}) = P(\phi^2_{m_2})$ $(\equiv P(\phi_m))$ are satisfied at $t = 0$.

The one-mode photon-number distributions $P(n)$ [(TC-1n) and (TSV-1n)] and one-mode photon-phase distributions $P(\phi)$ [(TC-1p) and (TSV-1p)] are shown in our previous articles [23–29, 38]. It was found that the distribution $P(n)$ for the TC field exhibits Poisson distribution, while the distribution $P(n)$ of TSV coincides with the distribution for a thermal field. It is also known that the distribution $P(\phi)$ of TC exhibits a single sharp peak around $\phi = 0$, while the TSV exhibits a uniform one-mode photon distribution $P(\phi)$, which represents a mixed state composed of random-phase components and is equal to that of the thermal field.

### DYNAMICS OF DIAGONAL MOLECULAR DENSITY MATRICES

In this section, we investigate the dynamics of diagonal density matrix (population) of each state [the ground state (**1**), the first excited state (**2**), and the second excited state (**3**)] of the molecule for the two types of two-mode fields (TC) and (TSV) with several frequencies [Fig. 2 (TC-d-a)-(TC-d-d) and (TSV-d-a)-(TSV-d-d)]. For TC-d-a, both one- and two-photon processes contribute to the dynamics because this model satisfies both one- and two-photon resonance conditions. In this model, there are shown to be two types of collapse and revival behaviors. The first revival–collapse behavior with smaller amplitudes is found to be mainly contributed by the one-photon process between states **1**

and **2**, while the second one with larger amplitudes is found be mainly done by the two-photon process between states **1** and **3**. The increase in the one-photon detuning with respect to state **2** [see Fig. 2 (TC-d-b)-(TC-d-d)] leads to the relative decrease in the diagonal density of state **2** ($\rho_{2,2}$), the feature of which represents the relative increase in the two-photon contribution between states **1** and **3** (see $\rho_{1,1}$ and $\rho_{3,3}$). It is also found that the revival time increases and the amplitude of oscillations is reduced as increasing the detuning. This feature can be understood by the decrease in the speed of the photon-phase splitting, which is ascribed to be the decrease in the interaction between the molecule and the photon field in the one-photon process [25, 26, 42].

In contrast, for TSV-d-a, the diagonal density matrix of each state exhibits a random oscillation like a thermal field [33]. The increase in the one-photon detuning with respect to state **2** is found to cause the resurrection of periodic oscillations in $\rho_{1,1}$ and $\rho_{3,3}$, which are related to the two-photon process. The origin of this behavior is found to be in the linear dependence of the Rabi frequency on the photon numbers in the large one-photon detuning, in which the photon statistical averages become sums of commensurate Rabi oscillations [33]. In our previous article [43], we also found that the only $|\rho_{1,3}|$ (representing the coherency between states **3** and **1**) is preserved with high values in the case of satisfying both one- and two-photon resonance conditions. Therefore, the effects of the increase in the one-photon detuning, which resurrects the periodic behaviors of diagonal density matrices, on the coherency between states **3** and **1** ($|\rho_{1,3}|$) is interesting. Before discussing the dynamics of off-diagonal density matrices, we investigate the dynamics of photon-phase sum and -difference distributions in the next section.

## DYNAMICS OF PHOTON-PHASE-SUM AND -DIFFERENCE DISTRIBUTIONS

We examine the dynamics of photon-phase-sum $P(\phi^+)(\equiv P(\phi^1 + \phi^2))$ and photon-phase-difference $P(\phi^-)(\equiv P(\phi^2 - \phi^1))$ distributions. Figures 3 and 4 show these distributions at several times, e.g., (I)–(VII) in Figure 2(TC-d-a), represented by dotted lines in Figure 2. Note that the distribution $P(\phi^+)$ corresponds to the sum of pure phase parts, whereas the distribution $P(\phi^-)$ includes the phase $[(\omega_2 - \omega_1)t]$ of the free field because the time $t$ is taken as $2\pi m/(\omega_1 + \omega_2)$ $(m = 0, 1, 2, \ldots)$ in this study. However, the changes in the shape of the distribution $P(\phi^-)$ can be elucidated by considering its $2\pi$-periodicity although the phase origin moves at each time due to the contribution of the free field.

It was already found that the splitting and colliding processes in the phase distribution are caused by the interaction between molecule and a coherent field and that their behaviors correspond to the collapse and revival behaviors in the molecular population, respectively [23–29, 38, 42]. However, because the splitting and colliding are not completely achieved in a larger time region due to the uncertainty relation between a photon phase and a photon number the collapse–revival behavior becomes unclear as time proceeds.

We first investigate the dynamics of distributions $P(\phi^+)$ and $P(\phi^-)$ of TC (Fig. 3). The initial $P(\phi^+)$ and $P(\phi^-)$ distributions for TC provide an identical single peak around $\phi^+ = \phi^- = 0$. For TC-a (satisfying both one- and two-photon resonance conditions), the first collapse behavior at times (I)–(III) is found to correspond to the broadening of the initial peak and the subsequent splitting into three peaks. The moving of the side peaks (in mutually opposite direction) of the distribution $P(\phi^+)$ and the colliding at times (III)–(VI) correspond to the quiescent region of the molecular population [Fig. 2 (TC-d-a)(III)–(VI)]. In contrast, the distribution $P(\phi^-)$ shows a more slowly splitting of the peak, which is understood by the fact that the phase sum $\phi^+$ has a larger frequency than the phase difference $\phi^-$. At time (IV), although the distribution $P(\phi^-)$ exhibits a broadened single peak the distribution $P(\phi^+)$ is shown to be split into two peaks, one of which is around $\phi^+ = 0$ and the other is around $\phi^+ = \pm\pi$. The phase difference between these two peaks is found to be about $\pi$, which corresponds to the situation of the $\pi/2$-difference between the side and main peaks observed in a one-mode field case [23, 24]. This implies that the TC at time (IV) hardly destroys the relative phase relation between molecular states **1** and **3**. This feature supports that the region around time (IV) for TC corresponds to a quiescent region [see Fig. 2 (TC-d-a)]. At time (VI), the split side peaks of the distribution $P(\phi^+)$ are shown to collide with the central peak around $\phi^+ = 0$ and then to become a broad single peak, the feature of which supports the beginning of the first revival with small amplitude around time (VI). At time (VII) (revival region with a maximum amplitude), the distribution $P(\phi^+)$ exhibits a nearly single peak with broad side peaks centered on $\phi^+ = \pm\pi$ although $P(\phi^-)$ exhibits two split peaks with a dif-

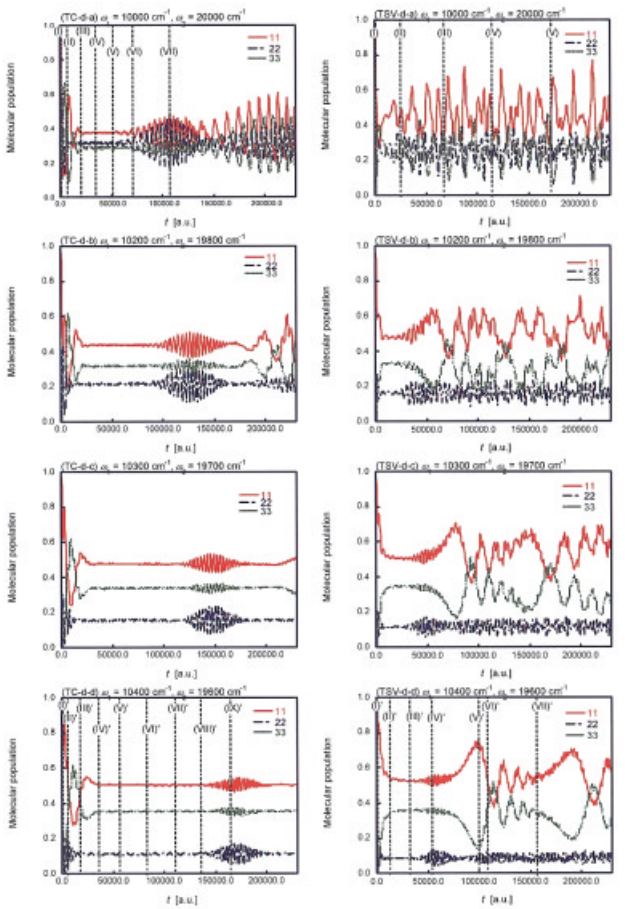

**FIGURE 2.** Time evolutions of the population ($\rho_{1,1}$, $\rho_{2,2}$, and $\rho_{3,3}$) of each state of the molecule (Fig. 1) for two-mode coherent field models TC-a–TC-d and two-mode squeezed vacuum field models TSV-a–TSV-d (see Fig. 1 legend). 11, 22, and 33 represent $\rho_{1,1}(t)$, $\rho_{2,2}(t)$, and $\rho_{3,3}(t)$, respectively.

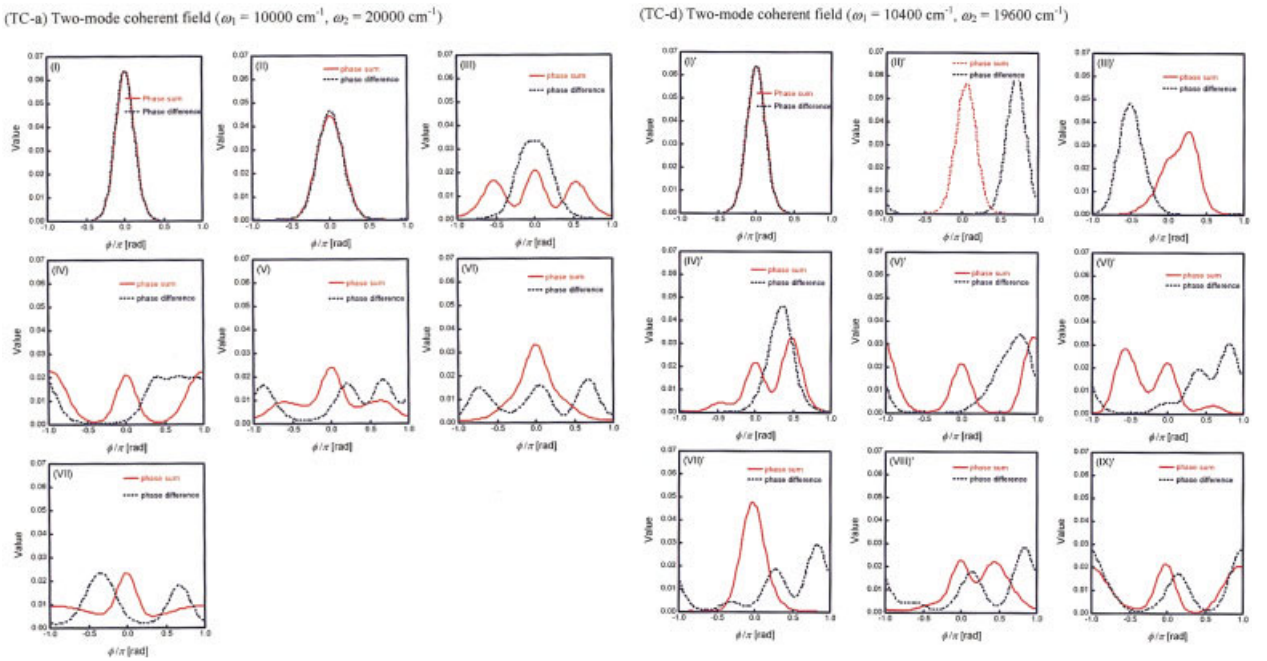

**FIGURE 3.** Photon-phase-sum and -difference distributions of two-mode coherent fields TC-a [at times (I)–(VII)] and TC-d [at times (I)′–(IX)′].

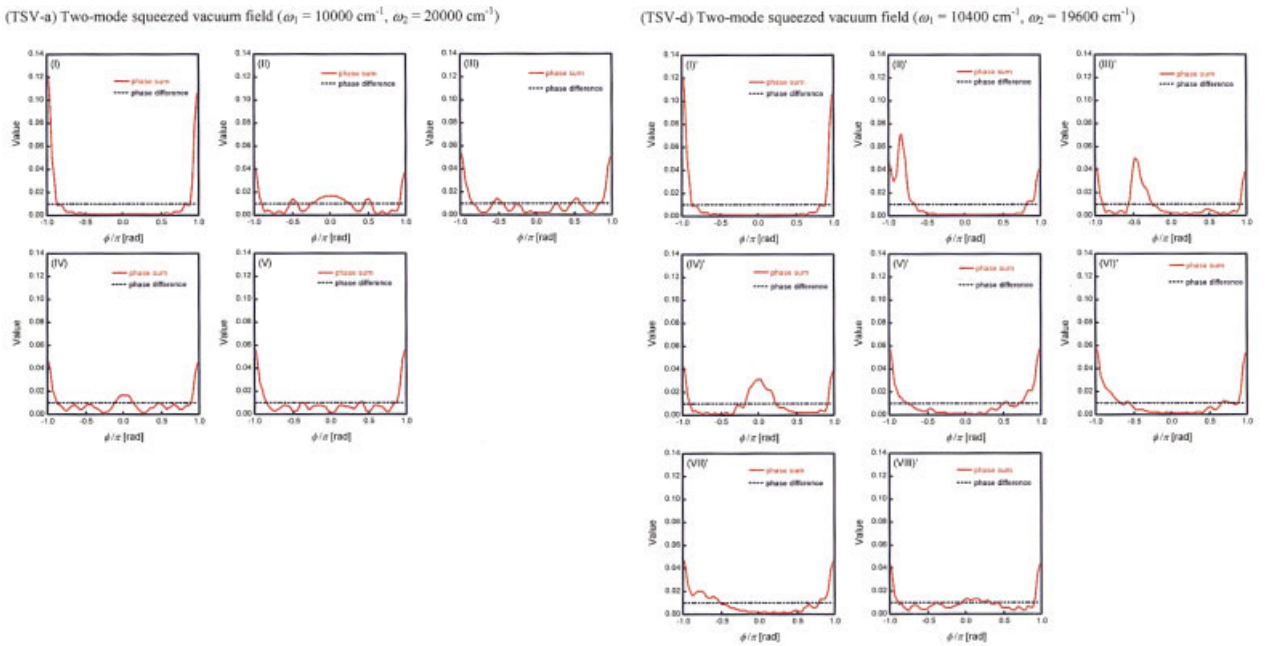


**FIGURE 4.** Photon-phase-sum and -difference distributions of two-mode squeezed vacuum fields TSV-a [at times (I)–(V)] and TSV-d [at times (I)′–(VII)′].

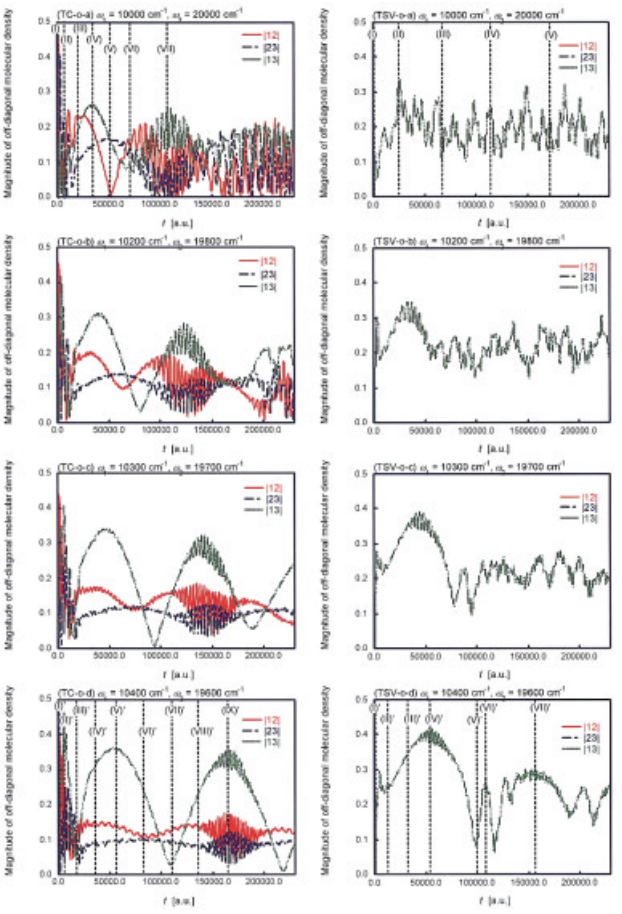


**FIGURE 5.** Time evolutions of the magnitudes of off-diagonal molecular density matrices, $|\rho_{12}(t)|$, $|\rho_{23}(t)|$, and $|\rho_{13}(t)|$, [(TC-o-a)-(TC-o-d) and (TSV-o-a)-(TSV-o-d)] for two-mode coherent fields TC-a–TC-d and two-mode squeezed vacuum fields TSV-a–TSV-d (see Fig. 1). 12, 23, and 13 represent $|\rho_{12}(t)|$, $|\rho_{23}(t)|$, and $|\rho_{13}(t)|$, respectively.

ference $\pi$, the feature of which hardly destroys the relative phase relation between the molecular states **1(2)** and **2(3)** in addition to that between states **1** and **3**. On the other hand, for TC-d (satisfying a two-photon resonant condition but not one-photon resonance condition) the splitting of distribution $P(\phi^+)$ is asymmetrical and the split side peaks are larger than those of TC-a, and the distribution $P(\phi^-)$ is more slowly split to three peaks with lower side peaks. This feature suggests that the contribution of the two-photon process becomes relatively large compared to the case of TC-a. The relation among molecular populations and phase distributions is found to be similar to that in the case of TC-a although the variation is slower, namely, the two split distributions $P(\phi^+)$ on $\phi^+ = 0$ and $\pm\pi$ and a broad single peak $P(\phi^-)$ at time (V)′ correspond to the quiescent region, and the latter similar distribution [but in this case $P(\phi^-)$ also splits to two peaks with a difference $\pi$] at time (IX)′ does to the revival region with a maximum amplitude.

We next investigate the dynamics of distributions $P(\phi^+)$ and $P(\phi^-)$ of (TSV) (Fig. 4). For TSV-a (satisfying both one- and two-photon resonance conditions), the $P(\phi^+)$ exhibits a single peak on $\phi^+ = \pm\pi$ at the initial time and only slight splitting and colliding behaviors are observed in later times, while $P(\phi^-)$ remains a uniform distribution like a thermal field. Such small splitting and colliding of $P(\phi^+)$ indicates that the one-photon contributions are larger than a two-photon contribution. This is also understood by the fact that two one-photon resonance conditions (molecular states **1–2** and **2–3**) are satisfied in TSV-a. As seen from the definition of TSV [Eq. (3)], the one-photon reduced density has the identical distribution with that of a thermal field, so that the $P(\phi^-)$ remains uniform and the population of each molecular state exhibits random oscillations like a thermal field [see Fig. 2 (TSV-d-a)]. In contrast, for TSV-d (only satisfying the two-photon resonance condition) distinct splitting and colliding of $P(\phi^+)$ are observed although $P(\phi^-)$ remains uniform. This feature is understood by the fact that the contribution of a two-photon process becomes relatively larger than those of one-photon processes due to the large one-photon detuning with respect to state **2**. Although slight two-photon detuning with respect to molecular state **3** causes the asymmetrical splitting and the off-resonant one-photon processes still destroy the coherency between states **1(2)** and **2(3)**, there is a similar relation among molecular populations ($|\rho_{11}|$ and $|\rho_{33}|$) and phase sum $P(\phi^+)$ to those observed in TC-d, namely, the split two peaks of $P(\phi^+)$ with a difference $\pi$ at time (IV)′ in Figure 3 (TSV-d) corresponds to a quiescent region shown in Figure 2 (TSV-d-d). The distribution at time (VIII)′ also provides a similar distribution to that at time (IV)′ although the central peak is much lower and obscure. This distribution corresponds to the more incomplete quiescent region at time (VIII)′. Judging from these results, the periodic behaviors emerging in TSV-d-d are similar to the collapse–revival behaviors in TC. To confirm this prediction, the dynamics of the magnitudes of off-diagonal molecular density matrices (representing the coherency between molecular states) are investigated in the next section.

## DYNAMICS OF OFF-DIAGONAL MOLECULAR DENSITY MATRICES

Figures 5 (TC-o-a)-(TC-o-d) and (TSV-o-a)-(TSV-o-d) show the dynamics of off-diagonal molecular density matrices for TC-a–TC-d and TSV-a–TSV-d fields, respectively. The magnitude of off-diagonal molecular density matrix ($|\rho^{\mathrm{mol}}_{i,j}|$) represents the degree of coherency (definite relative phase) between the states $i$ and $j$ of a molecule. It is found for TC that all the off-diagonal density matrices give similar magnitudes to each other in TC-o-a, while $|\rho^{\mathrm{mol}}_{1,3}|$ becomes much larger than $|\rho^{\mathrm{mol}}_{1,2}|$ and $|\rho^{\mathrm{mol}}_{2,3}|$ as the one-photon detuning increases [see Fig. 5 (TC-o-b)–(TC-o-d)]. It is also found that the distinct increase and decrease in all the off-diagonal density matrices are observed in the early time region in TC-o-a, while in the case of a large one-photon detuning, e.g., TC-o-d, the change in $|\rho^{\mathrm{mol}}_{1,3}|$ becomes more distinct and slower in contrast to those in other off-diagonal densities, which are significantly reduced. These features indicate the increase in the relative contribution of a two-photon process for those of one-photon processes in the case of the large one-photon detuning. For example, the local maxima of $|\rho^{\mathrm{mol}}_{1,3}|$ at times (IV) [(VII)] in TC-o-a and (V)′ [(IX)′] in TC-o-d correspond to the $\pi$-split distribution of $P(\phi^+)$ [see Fig. 3 (TC-a)(IV), (TC-a)(VII), (TC-d)(V)′, and (TC-d)(IX)′]. These features can be explained by the fact that the ability to destroy a relative phase between molecular states **1** and **3** is significantly reduced for the $\pi$-split distribution of $P(\phi^+)$.

In the case of TSV-o-a, only $|\rho^{\mathrm{mol}}_{1,3}|$ exists and is preserved with large values in the whole time region, the feature of which indicates the preservation of quantum coherency between molecular states **1** and **3**, although the molecular populations exhibit

random oscillations like a thermal field. Such behavior shows the coexistence of thermal and quantum features in the dynamics [43]. The preserved $|\rho_{1,3}^{\mathrm{mol}}|$ corresponds to the slight splitting of $P(\phi^+)$ in Figure 4 (TSV-a)(I)–(V), the feature of which is caused by the relatively large contribution of one-photon processes in TSV-a compared to that of two-photon process, which leads to the splitting of $P(\phi^+)$. On the other hand, in the case of TSV-o-d the distinct increase and decrease behaviors in $|\rho_{1,3}^{\mathrm{mol}}|$ emerge similarly to the case of TC-o-d. Actually, the maximum value of $|\rho_{1,3}^{\mathrm{mol}}|$ at time (IV)′ corresponds to the two split distributions of $P(\phi^+)$ with a difference $\pi$ at time (IV)′. Such distinct splitting and colliding of $P(\phi^+)$ are caused by the relative increase in the two-photon process between states **1** and **3**. However, because the one-photon distributions have completely random phases for TSV the slight detuning of the two-photon process causes asymmetrical splitting and colliding and a faster collapse of distinct distributions than the case of Figure 3 (TC-d). As a result, the periodic behaviors appearing in Figure 2 (TSV-d-d) are found to be similar to the collapse–revival behaviors in Figure 2 (TC-d-d) from the viewpoint of the dynamics of coherency between molecular states. This is a contrast to the fact that although similar periodic behaviors are also observed in the large one-photon detuning of the two-mode thermal field [33] all the off-diagonal molecular density matrices are predicted to completely vanish due to the random phases of the thermal field.

## Conclusion

We investigated the dynamics of a three-state molecular model interacting with two-mode coherent and two-mode squeezed vacuum fields in several cases of one-photon detunings under the two-photon resonance condition. As presented in our previous article [43], in the case of satisfying both one- and two-photon resonance conditions the two-mode squeezed vacuum field is shown to provide similar irregular oscillations of molecular populations to the case of a two-mode thermal field although the two-mode coherent field exhibits an explicit collapse–revival behavior of the molecular populations. The increase in the one-photon detuning with respect to molecular state **2** is found to cause the periodic behaviors of molecular populations ($\rho_{11}$ and $\rho_{33}$) in the case of a two-mode squeezed vacuum field. The off-diagonal molecular density matrix $|\rho_{13}|$ representing the coherency between molecular states **1** and **3** shows the distinctly large increase and decrease behaviors in TSV-o-d (with a large one-photon detuning) similarly to the case of TC-o-d. These behaviors are found to be related to the splitting and colliding behaviors of phase-sum distribution $P(\phi^+)$ of the two-mode photon fields. Consequently, the one-photon detuning of a two-mode squeezed field leads to the resurrection of periodic behaviors like a collapse–revival behavior, namely, in the case of a large one-photon detuning the distinct increase and decrease behaviors in $|\rho_{13}|$ emerge although in the case of satisfying both one- and two-photon resonance conditions the molecular coherency $|\rho_{13}|$ exhibits random oscillation with a high averaged value without distinctly large increase and decrease behaviors. This feature indicates that the slight frequency change in a two-mode squeezed vacuum field remarkably affects not only the dynamics of molecular populations but also the coherency between molecular states. Alternatively, a similar situation will be realized in the case of slight changes in the intermediate molecular states by utilizing the change in the intermolecular interaction (intermolecular distance) in molecular aggregates under the two-mode squeezed vacuum with fixed two-mode frequencies. The investigation toward such direction contributes to the direct control of the molecular coherency by changing both molecular (aggregate) properties and the quantum statistics of quantized photon fields. The results of such investigations will be also used in the creation of novel quantum dynamic phenomena in material science for quantum information devices in the future.

### ACKNOWLEDGMENT

This work was supported by Grant-in-Aid for Scientific Research 14340184 from the Japan Society for the Promotion of Science.

## References

1. Jaynes, E. T.; Cummings, F. W. Proc IEEE 1963, 51, 100.
2. Allen, L.; Eberly, J. H. Optical Resonance and Two-Level Atoms; Wiley: New York, 1975.
3. Knight, P. L.; Milonni, P. W. Phys Rep 1980, 66, 21.
4. Milonni, P. W.; Singh, S. Adv Atom Mol Opt Phys 1990, 28, 75.
5. Shore, B. W.; Knight, P. L. J Mod Opt 1993, 40, 1195.

6. Eberly, J. H.; Narozhny, N. B.; Sanchez-Mondragon, J. J. Phys Rev Lett 1980, 44, 1323.
7. Narozhny, N. B.; Sanchez-Mondragon, J. J.; Eberly, J. H. Phys Rev A 1981, 23, 236.
8. Knight, P. L.; Radmore, P. M. Phys Rev A 1982, 26, 676.
9. Hioe, F. T. J Math Phys 1982, 23, 2430.
10. Puri, R. R.; Agarwal, G. S. Phys Rev A 1986, 34, 3610.
11. Averbukh, I. S. Phys Rev A 1992, 46, R2205.
12. Góra, P. Ř.; Jedrzejek, C. Phys Rev A 1993, 48, 3291.
13. Góra, P. Ř.; Jedrzejek, C. Phys Rev A 1994, 49, 3046.
14. Góra, P. Ř.; Jedrzejek, C. Phys Rev A 1992, 45, 6816.
15. Gea-Banacloche, J. Phys Rev A 1993, 47, 2221.
16. Joshi, A.; Lawande, S. V. J Mod Opt 1991, 38, 1407.
17. Makhviladze, T. M.; Shelepin, L. A. Phys Rev A 1974, 9, 538.
18. Bogolubov, N. N. Jr.; Le Lien, F. ; Shumovski, S. Phys Lett 1984, 101A, 201.
19. Meshede, D.; Walther, H.; Müller, G. Phys Rev Lett 1985, 54, 351; Rempe, G.; Walther, H.; Klein, N. Phys Rev Lett 1987, 58, 353; Rempe, G.; Schmidt-Kaler, F.; Walther, H. Phys Rev Lett 1990, 64, 2783.
20. Chaba, A. N.; Collet, M. J.; Wall, D. F. Phys Rev A 1992, 46, 1499.
21. Cirac, J. I.; Blatt, R.; Parkins, A. S.; Zoller, P. Phys Rev Lett 1993, 73, 762; Cirac, J. I.; Blatt, R.; Parkins, A. S.; Zoller, P. Phys Rev A 1994, 49, 1202.
22. Bouwmeester, D.; Ekert, A.; Zeilinger, A., eds. The Physics of Quantum Information: Quantum Cryptography, Quantum Teleportation, Quantum Computation; Springer-Verlag: Berlin, 2000.
23. Nakano, M.; Yamaguchi, K. Chem Phys Lett 1998, 295, 317.
24. Nakano, M.; Yamaguchi, K. Chem Phys 2000, 252, 115.
25. Nakano, M.; Yamaguchi, K. Chem Phys Lett 1999, 304, 241.
26. Nakano, M.; Yamaguchi, K. J Phys Chem 1999, 103, 6036.
27. Nakano, M.; Yamaguchi, K. J Chem Phys 2000, 112, 2769.
28. Nakano, M.; Yamaguchi, K. Chem Phys Lett 2000, 324, 289.
29. Nakano, M.; Yamaguchi, K. Chem Phys Lett 2000, 317, 103.
30. Walls, D. W. Nature 1983, 306, 141.
31. Wehrl, A. Rev Mod Phys 1978, 50, 221.
32. Loudon, R.; Knight, P. L. J Mod Opt 1987, 34, 709.
33. Lai, W. K.; Buzek, V.; Knight, P. L. Phys Rev A 1991, 44, 6043.
34. Buzek, V.; Quang, T. J Opt Soc Am B 1989, 6, 2447.
35. Barnett, S. M.; Knight, P. L. J Opt Soc Am B 1985, 2, 467.
36. Takahashi, Y.; Umezawa, H. Collect Phenom 1975, 2, 55.
37. Israel, W. Phys Lett 1976, 57A, 107; Umezawa, H.; Johansson, A. E. I.; Yamanaka, Y. Class Quantum Grav 1990, 7, 385; Laflamme, R. Physica 1989, 158A, 58.
38. Nakano, M.; Yamaguchi, K. Phys Rev A 2001, 64, 033415-1-14.
39. Schumaker, B. L.; Caves, C. M. Phys Rev A 1985, 31, 3093.
40. Pegg, D. T.; Barnett, S. M. Phys Rev A 1989, 39, 1665.
41. Barnett, S. M.; Pegg, D. T. J Mod Opt 1997, 44, 225.
42. Eislet, J.; Risken, H. Phys Rev A 1991, 43, 346.
43. Nakano, M.; Yamaguchi, K. Chem Phys 2003, 286, 257.